



Contents lists available at ScienceDirect

Icarus

journal homepage: www.elsevier.com/locate/icarus

Rainfall on Noachian Mars: Nature, timing, and influence on geologic processes and climate history

Ashley M. Palumbo^{a,*}, James W. Head^a, Lionel Wilson^b

^a Department of Earth, Environmental and Planetary Sciences, Brown University, Providence, RI 02912, USA

^b Lancaster Environment Centre, Lancaster University, Lancaster LA1 4YQ, United Kingdom

ARTICLE INFO

Keywords:

Rainfall
Climate
Noachian
Erosion

ABSTRACT

The formation of martian geologic features, including degraded impact craters, valley networks, and lakes, has been interpreted to require a continuously “warm and wet” Noachian climate, with above-freezing surface temperatures and rainfall. More specifically, it has been argued that a change in the nature of rainfall in the Noachian, from a diffusive rain splash-dominated erosional regime to an advective runoff-dominated erosional regime, is the best explanation for the observed temporal differences of erosion style: the degradation of craters has been interpreted to be due to rain splash throughout the Noachian, while the formation of valley networks and lakes has been interpreted to be due to more erosive activity and more abundant fluvial activity at the Noachian/Hesperian transition. However, the presence of a long-lived “warm and wet” climate with rainfall is difficult to reconcile with climate models which instead suggest that the long-lived climate may have been “cold and icy”, with surface temperatures far below freezing, precipitation limited to snowfall, and most water trapped as ice in the highlands. In such a “cold and icy” climate scenario, fluvial and lacustrine activity would only be possible during transient warm periods, which could produce “warm and wet” conditions for relatively short periods of time. In this work, we (1) review the geomorphic evidence for Noachian rainfall and the various rainfall-related erosional regimes, (2) explore climate model predictions for a “cold and icy” climate and the potential for short-lived “warm and wet” excursions, and (3) attempt to characterize the transition from diffusive to advective erosional rainfall regimes through analysis of atmospheric pressure and rainfall dynamics with the goal of providing insight into the nature of the Noachian hydrological cycle and thus, the Noachian climate. We conclude that (1) if rainfall occurred on early Mars, raindrops would have been capable of transferring sufficient energy to initiate sediment transport regardless of atmospheric pressure, implying that rain splash would have been possible throughout the Noachian, and (2) in contrast to previous findings, maximum possible raindrop size does not depend on atmospheric pressure and, as a result, simple parameterized relationships suggest that rainfall intensity (rainfall rate) does not depend on atmospheric pressure. Therefore, our results, based on the implementation of a simple parameterized relationship for rainfall intensity, predict that there would not have been a transition from rain splash-dominated erosion to runoff-dominated erosion related solely to decreasing atmospheric pressure in the Noachian. This finding is not consistent with the hypothesis of Craddock and Lorenz (2017) that the long-lived Noachian climate was “warm and wet” with rainfall throughout the Noachian and that rainfall intensity changed as a function of atmospheric pressure declining through time; our findings do not preclude the possibility that early Mars was predominantly “cold and icy”. Remaining unknown is the mechanism(s) for the observed geomorphic transition in erosion style, and whether melting of surface snow/ice and runoff during a punctuated heating episode in an otherwise “cold and icy” climate could explain the formation of the valley networks and lakes in the absence of rainfall. We conclude by outlining future work that introduces more advanced methodology to further explore a possible relationship between rainfall intensity and atmospheric pressure.

* Corresponding author.

E-mail address: Ashley_Palumbo@Brown.edu (A.M. Palumbo).

<https://doi.org/10.1016/j.icarus.2020.113782>

Received 26 February 2020; Accepted 26 March 2020

Available online 11 April 2020

0019-1035/© 2020 Elsevier Inc. All rights reserved.

1. Introduction

Observations of martian surface features, including the valley networks (e.g. Fassett and Head, 2008a; Hynek et al., 2010) and open- and closed-basin lakes (e.g. Cabrol and Grin, 1999; Fassett and Head, 2008b; Goudge et al., 2015), indicate that overland fluvial flow and lacustrine activity occurred in the Late Noachian-Early Hesperian era (LN-EH, ~3.7 Ga) (Fassett and Head, 2008a). Evidence suggests that this fluvial and lacustrine activity was most intense in the LN-EH; the majority of valley networks and lakes are on LN-EH-aged terrains (Fassett and Head, 2011). This implies that the nature of the climate and erosional regime in the LN-EH was much different from the nature of the climate and erosional regime both earlier in the Noachian and later in the Hesperian and Amazonian (Howard et al., 2005; Irwin et al., 2005), with the LN-EH interpreted to have been characterized by relatively more rainfall and overland flow (e.g. Craddock and Howard, 2002; Ramirez and Craddock, 2018). However, overland flow, a potentially effective form of advective erosion (sediment transport and erosion due to movement via currents of fluid movement), is not the only signature of liquid water activity on the early Martian surface: Noachian-aged impact craters commonly have degraded rims, shallow floors, and lack visible ejecta deposits and central peaks, features that cannot easily be explained without the influence of diffusive erosion (Craddock and Howard, 2002) in addition to advective erosion. Interestingly, younger Hesperian or Amazonian-aged craters do not display these characteristics. Researchers have postulated that rain splash, an effective form of diffusive erosion, was important in the Noachian and was predominantly responsible for the observed crater degradation (e.g. Craddock and Howard, 2002); rain splash is a diffusive process through which sediment transport is initiated by the collision of raindrops with the surface. Many other forms of advective and diffusive erosion exist, such as aeolian erosion, mass wasting, or micrometeorite bombardment.

However, rainfall-related mechanisms, including rain splash and overland flow, are interpreted to be the only diffusive and advective erosional mechanisms that are effective enough to leave the observed surficial expression and are not expected to have continued into the Hesperian and Amazonian (Craddock and Howard, 2002). It is important to note that Craddock and Howard (2002) discuss other possible explanations for these characteristics of crater morphology, including solifluction as the dominant diffusional process and surface runoff from snowmelt, but they find that rain splash and rainfall-driven runoff is the “simplest way of explaining” their observations (Craddock and Howard, 2002).

Thus, the paradigm for Noachian erosion follows: diffusive erosion from rain splash is interpreted to have been dominant throughout most of the Noachian, leading to the degradation of crater rims and erosion of ejecta deposits, and advective erosion from rainfall and surface runoff is interpreted to have been dominant at the LN-EH boundary, leading to the formation of the valley networks and lakes (e.g. Craddock and Howard, 2002; Craddock and Lorenz, 2017). In addition to this role of rainfall, some valley networks are sourced from lakes and required lake overspill to form, suggesting the presence of abundant liquid water on the surface in the LN-EH. In this paradigm for martian erosion, at later times throughout most of the Hesperian and Amazonian, temperatures are interpreted to have been too cold to permit rainfall, thereby explaining the absence of degraded craters, valley networks, and lakes on these younger terrains (e.g. Craddock and Howard, 2002).

To explain these erosional regimes and the persistence of rainfall in the Noachian and LN-EH, researchers commonly call upon the hypothesis that the early martian climate was “warm and wet” (e.g. Craddock et al., 1997, 2018; Craddock and Howard, 2002; Craddock and Lorenz, 2017), characterized by global mean annual temperature (MAT) above freezing and rainfall (Ramirez and Craddock, 2018) (Fig. 1). Note that this “warm and wet” climate may have been arid to semi-arid in

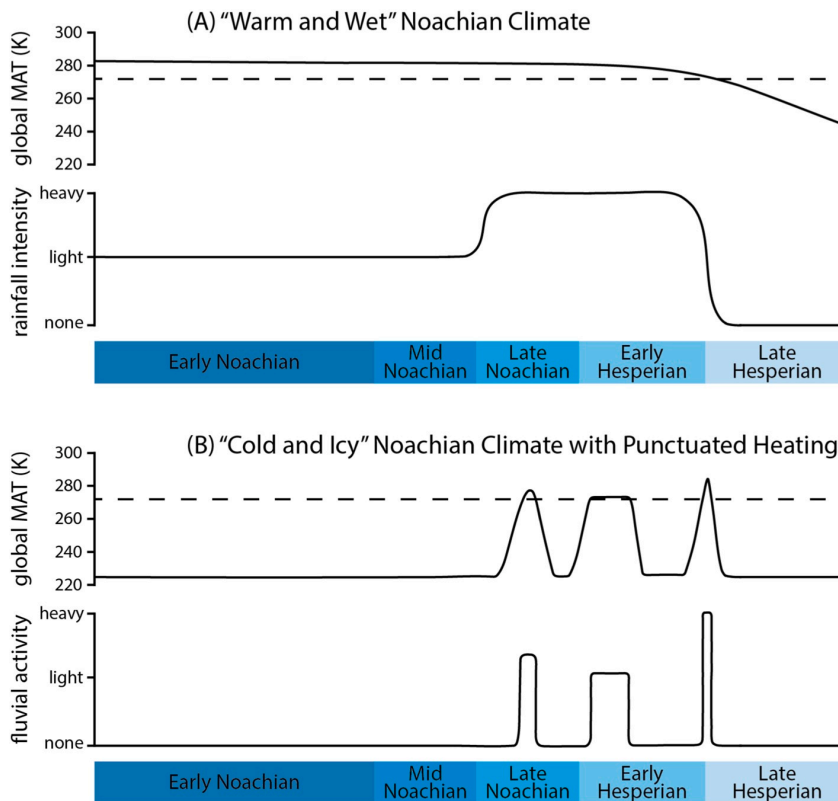


Fig. 1. Schematic diagram of relationship between global MAT, rainfall intensity/fluvial activity, and time for the case of (A) a long-lived “warm and wet” climate, slowly cooling through time as the atmosphere is lost, and (B) a long-lived “cold and icy” climate with periods of punctuated heating in the LN-EH. Horizontal dashed line is at 273 K. The units for rainfall intensity and fluvial activity are ‘none’, ‘light’, ‘heavy’ and are purposefully non-descript as we aim to only place relative estimates in this schematic diagram. For reference, the Early Noachian began ~4.1 Ga when Hellas basin formed, the Late Noachian-Early Hesperian boundary occurs ~3.7 Ga, and the Late Hesperian ended ~3 Ga. Punctuated heating events in a long-lived “cold and icy” climate are illustrated here as spikes in temperature. The magnitude and duration of a punctuated heating event would depend on the mechanism causing the heating; we have illustrated a range of different possibilities and are not referencing one specific heating mechanism. The number of required punctuated heating events is also not well-constrained and may have been only a few or many. Note that more intense (higher temperature) punctuated heating events would have led to more intense melting and fluvial activity.

comparison with Earth; however, relatively more rainfall is expected to have occurred in the Noachian (especially in the Late Noachian) than at other times during martian history. The abundance and rates of rainfall (rainfall intensity) are expected to have changed throughout the Noachian, causing the shift from a diffusive rainfall-related erosional regime (rain splash and infiltration; crater degradation) to an advective rainfall-related erosional regime (runoff and fluvial erosion; valley networks and lakes) (Craddock and Lorenz, 2017).

In contrast to this evidence for warm temperatures and rainfall, climate modeling studies (e.g. Forget et al., 2013; Kasting, 1991; Wordsworth et al., 2013) have not been able to successfully reproduce long-lived (e.g. spanning the Noachian era) “warm and wet” conditions on early Mars. Due to the influence of the faint young Sun, these recent models instead predict that the long-lived background Noachian climate was “cold and icy”, characterized by temperatures far below freezing (global mean annual temperature, MAT, ~225 K) and with most surface water trapped as snow and ice in the highlands. In this “cold and icy” climate scenario, fluvial and lacustrine activity would only be possible during periods of punctuated or transient heating, which could have produced short-lived “warm and wet” conditions (e.g. conditions suitable to melting and runoff or rainfall and runoff), for example, in the LN-EH (Fig. 1).

Analysis of the predicted nature and persistence of these two erosional regimes in the Noachian may provide important insight into whether the climate was continuously “cold and icy” (with periods of punctuated heating to permit fluvial activity) or “warm and wet” (with rainfall throughout the Noachian, but varying in rate and intensity as a function of time). In this contribution, we revisit the nature and evolution of the early martian climate through an analysis of rainfall-related processes in an effort to understand the link between the geomorphic observations and the characteristics of the early climate. Specifically, we (1) review the geomorphic evidence for rainfall in the Noachian and the various rainfall-related erosional regimes, (2) explore predictions from some recent climate modeling studies regarding the characteristics of the Noachian climate and the potential for short-lived “warm and wet” excursions in an otherwise “cold and icy” climate, (3) attempt to characterize the transition from a diffusive to an advective erosional regime through mathematical relationships in an effort to link the geology with climate model predictions, and (4) conclude by outlining outstanding questions and potential avenues of future research.

2. Rainfall in the Noachian: predictions based on geomorphology

Craters of different ages (spanning the Noachian era) are preserved in various stages of degradation, implying that erosive activity was operating nearly continuously throughout the Noachian (Craddock et al., 1997; Craddock and Howard, 2002). Specifically, older Noachian craters have experienced more erosion than younger Noachian craters (e.g. Craddock et al., 1997; Craddock and Howard, 2002; Forsberg-Taylor et al., 2004; Howard, 2007; Jones, 1974) and smaller diameter craters appear to have eroded more quickly than larger diameter craters (Craddock et al., 1997). Rainfall is likely to have played an important role in the observed erosion, including degradation of crater rims, shallowing of crater floors, and erosion of ejecta deposits (e.g. Craddock and Howard, 2002). Specifically, diffusive activity from rain splash may be required to explain the observed crater degradation (e.g. Craddock and Howard, 2002). It is important to note that other additional erosive activity may be required to explain the observed crater-related erosion in its entirety, including the possible role of some forms of advective erosion, such as backwasting (Forsberg-Taylor et al., 2004). In addition to this, valley networks and lakes imply that a predominantly advective erosional regime, with surface runoff and fluvial activity, was important in the LN-EH (e.g. Howard et al., 2005; Irwin et al., 2005).

This geologic evidence for rainfall and various rainfall-related processes, including rain splash and overland flow, that were shaping the

surface in the Noachian has led researchers to postulate that there were two different aqueous rainfall-related erosional regimes in the Noachian (e.g. Craddock and Howard, 2002; Craddock and Lorenz, 2017). First, the rainfall-related erosional regime in the Early-to-Mid Noachian is interpreted to have been dominated by diffusive processes, specifically rain splash. In this rain splash-dominated erosional regime, rainfall rates were generally too low to exceed the infiltration capacity of the regolith; most rainfall infiltrated into the subsurface, surface runoff was minimal or negligible, and rainfall-related erosion was mostly diffusive (e.g. Craddock and Howard, 2002). Second, and subsequently, the rainfall-related erosional regime in the LN-EH is interpreted to have been dominated by advective processes, specifically surface runoff and overland flow. In this runoff-dominated regime, rainfall rates were sufficiently high such that rainfall exceeded the infiltration capacity of the regolith and runoff occurred (e.g. Craddock et al., 1997; Craddock and Howard, 2002; Howard, 2007). Rain splash erosion is still expected to have occurred, but the dominant rainfall-related erosive mechanism was surface runoff. This shift in rainfall-related erosional regime through time is interpreted to be consistent with (1) the increasing degree of degradation of Noachian craters as a function of age and (2) the presence of the LN-EH valley networks and lakes (e.g. Craddock et al., 1997; Craddock and Howard, 2002). Prior to the LN-EH, erosion was more effective than in the current Amazonian regime, albeit less effective than in the LN-EH: in the Early- to Mid-Noachian, rain splash acted to degrade crater rims and effectively remove ejecta deposits, and in the LN-EH, more intense rainfall was responsible for enhanced crater erosion and formation of the observed fluvial and lacustrine features (e.g. Craddock and Lorenz, 2017). In summary, “A change in the nature of rainfall during the history of early Mars appears to be the best solution for the observed temporal differences between the style of erosion during the Noachian as represented by modified impact craters (e.g. Craddock and Howard, 2002) followed by more enhanced erosion during the Noachian/Hesperian transition as typified by valley networks (Fassett and Head, 2008a; Howard, 2007; Howard et al., 2005; Irwin et al., 2011; Matsubara et al., 2013)” (Craddock and Lorenz, 2017). Thus, this geomorphic hypothesis provides important predictions regarding the required climatologic characteristics of the Noachian that can be explored further with climate models.

3. Rainfall in the Noachian: predictions based on climate models

Modeling studies of the early martian climate suggest that the long-lived background Noachian climate was more likely to have been “cold and icy” than “warm and wet” (e.g. Forget et al., 2013; Kasting, 1991; Wordsworth et al., 2013). In the Noachian, if atmospheric pressure exceeded a few tens of millibars, many recent 3-dimensional global climate models (GCMs) predict that the surface and atmosphere would have been thermally linked together, producing an adiabatic cooling effect and causing temperature variations to have been dominantly dependent on altitude, rather than latitude (e.g. Forget et al., 2013). In a “cold and icy” climate scenario, global MAT is predicted to have been ~225 K and, because of the adiabatic cooling effect, most surface water is predicted to have been trapped in the highlands as snow and ice. Temperatures are predicted to have been far too cold for rainfall to occur and, thus, it is difficult to reconcile these Noachian rainfall-dominated erosional regimes with results from recent climate models (e.g. Forget et al., 2013; Wordsworth et al., 2013, 2015).

Several studies have focused on how to reconcile the advective rainfall-related LN-EH erosional regime, which is interpreted to be required to explain the valley networks and lakes, with this “cold and icy” climate scenario. Some researchers have suggested that LN-EH fluvial and lacustrine activity, driven by rainfall and/or snowmelt, could have occurred during periods of punctuated heating (e.g. Head and Marchant, 2014; Wordsworth, 2016). There may have been specific punctuated heating events in the LN-EH that produced short-lived

“warm and wet” conditions in an otherwise “cold and icy” climate regime, potentially explaining the peak in advective erosion (Fig. 1). Some researchers refer to this as a ‘climatic optimum’ (for additional evidence for and discussion of mechanisms that could cause this climatic optimum, see Howard et al., 2005; Irwin et al., 2005; Howard, 2007).

Multiple LN-EH punctuated/transient heating mechanisms have been proposed, including impact cratering-induced heating (e.g. Palumbo and Head, 2018b; Segura et al., 2008; Toon et al., 2010), volcanism-induced heating (e.g. Halevy and Head, 2014; Johnson et al., 2008; Kerber et al., 2015; Mischna et al., 2013), spin-axis/orbital variations and summertime melting (e.g. Kite et al., 2013; Mischna et al., 2013; Palumbo et al., 2018), transient greenhouse-rich atmospheres (e.g. Wordsworth et al., 2017), and the presence of high-altitude clouds (e.g. Forget and Pierrehumbert, 1997; Segura et al., 2008; Urata and Toon, 2013). We identify these as ‘punctuated’ or ‘transient’ heating mechanisms because the associated heating would have occurred for a finite period of time shorter than the duration of the LN-EH era, ranging from days to hundreds of thousands of years (note that other mechanisms have also been proposed which could have led to warm periods of up to ~10 million years in duration, such as climate cycling forced by the carbonate-silicate cycle; Batalha et al., 2016). Studies of the heating potential of each of these punctuated heating mechanisms have shown that the most likely candidates to have been sufficiently active in the LN-EH to have increased global MAT to >273 K in a long-lived background “cold and icy” climate are transient greenhouse-rich atmospheres and the presence of high-altitude water clouds. In this section, we review these two punctuated heating mechanisms to determine whether short-lived “warm and wet” conditions could have persisted in a long-lived background “cold and icy” climate and, further, whether abundant rainfall, surface runoff, and advective erosion is expected to have occurred during these transient warm excursions.

3.1. Transient greenhouse-rich atmospheres

When considering reasonable source and sink constraints, many greenhouse gases are incapable of producing sufficient greenhouse warming on early Mars (e.g. see review by Forget et al., 2013). However, recent work has shown that, while methane and hydrogen alone are not strong greenhouse gases, collision induced absorption (CIA) effects lead to new and stronger absorptions (e.g. Wordsworth et al., 2017). Ongoing work aims to constrain the magnitude of associated heating and concentration of these gases that are required to increase global MAT to >273 K on early Mars (e.g. Ramirez et al., 2014; Turbet et al., 2019; Wordsworth et al., 2017), but preliminary results suggest that it is possible with reasonable concentrations of H₂ or CH₄ (Wordsworth et al., 2017). This punctuated heating mechanism could have occurred in the LN-EH; H₂ and CH₄ could have been introduced to the atmosphere through volcanism (e.g. Ramirez, 2017; Ramirez et al., 2014), or serpentinization (e.g. Holm et al., 2015) and/or clathrate breakdown (Kite et al., 2017), respectively.

3.2. High-altitude clouds

Given the correct cloud characteristics, including cloud height, clouds can scatter IR radiation back towards the surface, producing a greenhouse effect. Researchers have hypothesized that high-altitude CO₂ clouds (e.g. Forget and Pierrehumbert, 1997) and high-altitude H₂O clouds (e.g. Segura et al., 2008; Urata and Toon, 2013; for additional modeling studies of the effects of high altitude H₂O clouds, see Madeleine et al., 2012, 2014) could have significantly heated the early martian surface. However, recent 3D GCM studies have shown that (1) high-altitude CO₂ ice clouds can only bring sufficient heating if there is ~100% cloud coverage (e.g. Forget and Pierrehumbert, 1997; Mischna et al., 2000), which is unlikely (Forget et al., 2013; Wordsworth et al., 2013), and (2) heating associated with high-altitude H₂O clouds can increase global MAT to >273 K for centuries or longer (Mischna et al.,

2019), but these clouds can only form in very arid conditions (Urata and Toon, 2013; Kite et al., 2019) and require very low precipitation rates (Urata and Toon, 2013).

3.3. Characteristics of a transiently-heated climate

In order to determine whether abundant rainfall and surface runoff is expected to have occurred during these periods of transient or punctuated heating, some researchers have used climate models to explore the characteristics of greenhouse-heated and high-altitude cloud-heated climates.

First, we review the model-predicted characteristics of greenhouse-heated climates. Palumbo and Head (2018a) used a 3D GCM to simulate a greenhouse-heated atmosphere by using gray gas as a proxy for greenhouse heating. Interestingly, for climates with global MAT ~275 K, above the melting point of water and consistent with the canonical view of a “warm and wet” climate (e.g. Ramirez and Craddock, 2018), (1) the highest elevation regions, including parts of the Tharsis rise, are below freezing year-round and act as surface cold traps for water, (2) precipitation is dominated by snowfall, and (3) rainfall is negligible (Palumbo and Head, 2018a). It is important to note that Wordsworth et al. (2015) showed that rainfall is possible in an ‘above-freezing’ climate scenario (global MAT ~283 K, similar to the MAT on present-day Earth, ~288 K) with an oceanic water source in the northern lowlands. However, the presence of oceans is uncertain, particularly in the Noachian (e.g. Head et al., 2018), and the model-predicted distribution of rainfall is not well-correlated with the distribution of valley networks (Wordsworth et al., 2015).

Next, we review the model-predicted characteristics of high-altitude H₂O cloud-heated climates. We do not discuss high-altitude CO₂ cloud-heated climates here because 100% cloud coverage is required to bring sufficient heating and is unlikely (e.g. Forget et al., 2013). Urata and Toon (2013) used a 3D GCM and showed that specific conditions are required to produce high-altitude H₂O clouds and associated warm temperatures (above ambient, but not necessarily above freezing): (1) ice crystal sizes around 10 μ or larger, which is consistent with thin cirrus clouds on Earth, (2) low conversion rate of clouds to precipitation which is required to increase the lifetime of water in the atmosphere and permit the formation of thicker clouds (note that this did not naturally occur in their simulations; Urata and Toon (2013) had to force such low precipitation rates), (3) near ~100% cloud coverage to effectively reduce the cloud albedo which, although potentially consistent with thin cirrus clouds on Earth, has been suggested to be unlikely for early Mars (e.g. Forget et al., 2013), and (4) the surface must be inherently dry with limited surface water reservoirs. More recently, Kite et al. (2019) and Mischna et al. (2019) used a 3D GCM to explore the formation of high-altitude H₂O clouds on early Mars and found that it is only possible in very arid conditions, which is consistent with the earlier findings of Urata and Toon (2013). Even for global MAT ~290 K, the small amount of available surface water is cold-trapped in the highest elevation areas of the Tharsis rise and, as a result, rainfall is predicted to be negligible (e.g. Kite et al., 2019; Mischna et al., 2019). Note that the warm case from Urata and Toon (2013), their case 17 in table 3, does not find stable/equilibrated global MAT >273 K, even though the initial starting condition is global MAT ~300 K; instead they find that “the globally averaged surface temperature is several degrees below the melting temperature of ice, but several areas of the planet, including the Hellas region and the tropics, have annually averaged temperatures near melting”.

It is important to note that, because topography was the dominant control on the Noachian climate, the above results are dependent upon the topography that is implemented into the models. These works used present-day topography in their simulations, which is consistent with the major volcanic rises and impact basins having formed by the LN-EH (Fassett and Head, 2011). However, recent studies have suggested that the Tharsis rise may have been largely emplaced after the LN-EH (e.g.

Bouley et al., 2018), and thus a better understanding of Noachian topography may improve upon the accuracy of model-predicted characteristics of the early climate.

In summary, these transient “warm and wet” climates (which may have occurred due to punctuated/transient heating events in a long-lived, background “cold and icy” climate) do not appear to have been characterized by rainfall. Thus, if the LN-EH valley networks and lakes were formed during a period of transient heating in a long-lived “cold and icy” climate, we conclude that either (1) the transient warm climate was warmer than those simulated by Palumbo and Head (2018a) (e.g. global MAT >275 K), removing any surface cold traps and potentially permitting rainfall, (2) a different, currently unidentified, transient heating mechanism exists that causes rainfall, potentially through the introduction of large amounts of water vapor to the atmosphere, or (3) the observed fluvial and lacustrine activity was not caused by rainfall and runoff, but by snow/ice melting and runoff. Alternatively, the climate models that predict “cold and icy” conditions, albeit being the most up-to-date, complex, and physically self-consistent, do not perfectly capture the atmospheric physics, the long-lived Noachian climate was actually “warm and wet”, not “cold and icy”, and rainfall was continuous throughout the Noachian.

Additionally, it is important to note that rainfall and related processes occurring throughout the Noachian, as required by the proposed diffusive erosion mechanism of rain splash (e.g. Craddock et al., 1997; Craddock and Howard, 2002), are not consistent with a continuous and long-lived “cold and icy” climate with punctuated/transient heating in the LN-EH; all precipitation would be snowfall in a “cold and icy” climate, not rainfall. If the long-lived background climate was “cold and icy”, then this signature of diffusive erosion throughout the Noachian must be explained by other mechanism(s). One explanation for this could be one or more episodes of transient/punctuated heating throughout the Noachian that produced some rainfall, but not runoff, causing period(s) of diffusive erosion by rain splash. Alternatively, the observed erosion may have been caused by snowmelt and runoff, not rainfall and runoff (e.g. Fastook and Head, 2015; Palumbo and Head, 2018a).

4. Determining whether the nature of the rainfall-related erosional regime depends on atmospheric pressure

How, then, can we explain the erosional regimes that are required to account for the widespread Noachian-aged degraded craters and LN-EH valley networks and lakes? Are different erosional regimes caused by changing rainfall intensity as a function of decreasing atmospheric pressure? Further, what approach can be undertaken in order to

reconcile the geologic signature of rainfall with the climate models that apparently cannot reproduce conditions with abundant rainfall? Recent work utilized measurements of fossilized raindrop imprints in conjunction with equations for the relationship between raindrop velocity and atmospheric pressure in order to estimate the atmospheric pressure on early Earth (Kavanagh and Goldblatt, 2015; Som et al., 2012). Craddock and Lorenz (2017) called upon this type of methods to provide insight into the evolution of the early martian atmosphere and the process(es) that could have been responsible for the changing nature of rainfall. On the basis of basic equations and relationships, the authors hypothesized that the long-lived Noachian climate was “warm and wet”, with above-freezing temperatures and rainfall, and that the rainfall erosional regime could have shifted from rain splash-dominated to runoff-dominated as a function of decreasing atmospheric pressure through time (Craddock and Lorenz, 2017) as the atmosphere was slowly being lost to space (Fig. 2). Specifically, Craddock and Lorenz (2017) found that (1) rain splash-related erosion may not be possible for atmospheric pressures >4 bar, (2) rainfall intensity sufficient to cause surface runoff cannot exist for atmospheric pressures <~1.5 bar, and (3) lighter rain is more probable for higher atmospheric pressures, ~3–4 bar, which is more consistent with a rain splash-dominated erosional regime, and heavier rain is more probable for lower atmospheric pressures, ~1.5 bar, which is more consistent with a runoff-dominated erosional regime. These conclusions suggest that multiple rainfall regimes could have existed as atmospheric pressure declined through time, which Craddock and Lorenz (2017) interpreted to be generally consistent with the evidence for both diffusive and advective rainfall-related erosional regimes in the Noachian.

In this section, we revisit the mathematical equations and relationships which relate rainfall to atmospheric properties (following the general approach of Som et al., 2012; Craddock and Lorenz, 2017) in order to test the hypothesis that different erosional regimes could have existed under different atmospheric pressure regimes. This test provides insight into the plausibility of the long-lived Noachian climate being “warm and wet” with continuous rainfall, because the changing nature of rainfall and fluvial activity throughout the Noachian is predicted to have been controlled by decreasing atmospheric pressure (Craddock and Lorenz, 2017). Although this does not explain the required persistence of warm temperatures that cannot be reproduced by current climate models, it may explain the physical mechanism for the interpreted shift in erosional regime. Alternatively, if this shift in erosional regime cannot be explained by different atmospheric pressure regimes, we consider that an alternate explanation for the different erosional regimes must exist; such an alternative explanation may not require a long-lived “warm and wet” climate. By improving our understanding of the role

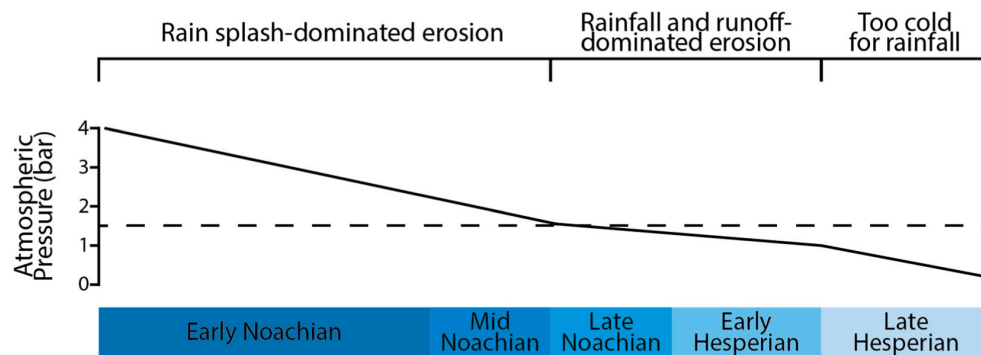


Fig. 2. Schematic diagram of the relationship between time, atmospheric pressure and erosional regime as proposed by Craddock and Lorenz (2017). In the Early-to-Mid Noachian, atmospheric pressure was above 1.5 bar but <4 bar, which is consistent with rain splash-dominated erosion (further, a recent study suggests that atmospheric pressure was <2 bars by the Middle Noachian; Warren et al., 2019). In the LN-EH, atmospheric pressure is <1.5 bar but high enough to still permit temperatures above 273 K (for the purpose of this illustration, we draw the lower limit for LN-EH atmospheric pressure at ~1 bar), which is consistent with runoff-dominated erosion. Throughout the Late Hesperian and Amazonian, atmospheric pressure is too low for temperatures to be above 273 K and rainfall does not occur.

that atmospheric evolution has on rainfall intensity and erosional regime, we strive to place tighter constraints on the predicted conditions that climate models must reproduce. To do this, we introduce the mathematical relationships for (1) the energy transfer from raindrops colliding with the martian surface, which provides important information about raindrop velocity, and, from there, (2) the maximum stable raindrop size capable of passing through the Martian atmosphere. Then we discuss the implications of our findings for rainfall intensity and different erosional regimes.

The energy transferred as a raindrop collides with the martian surface can be approximated by assuming that all of the kinetic energy of the falling raindrop is transferred to the surface upon collision, potentially initiating sediment movement. The kinetic energy, E , is equal to $0.5 m v^2$ where m is the mass of the raindrop and v is its velocity. Assuming a spherical raindrop (a good approximation for all but the largest raindrops, e.g., Craddock and Lorenz, 2017; Som et al., 2012) of diameter d , the mass is equal to $(\pi/6) d^3 \rho_{\text{water}}$ where ρ_{water} is the density of the raindrop. The simplest possible analysis would assume that any raindrop reaching the surface had attained its terminal velocity, v_b , defined as the maximum velocity that a raindrop can reach due to the balance between the gravitational and drag forces acting on it. The terminal velocity defined in this way is found by equating the weight of the drop, mg , where g is the acceleration due to gravity, to the drag force exerted on the raindrop by the atmosphere, $0.5 \rho_a C_d (\pi/4) d^2 v_t^2$, where ρ_a is the atmospheric density and C_d is a drag coefficient of order unity. Thus, the terminal velocity is given by:

$$v_t = \left(4 d \rho_{\text{water}} g / 3 C_d \rho_a \right)^{1/2}$$

and, hence, the kinetic energy, E , of a raindrop that is traveling at terminal velocity is given by

$$E = \frac{1}{9} \frac{\rho_{\text{water}}^2 g}{C_d \rho_a} \pi d^4$$

Given these assumptions, the relationships between raindrop diameter, d , terminal velocity, v_t , and kinetic energy, E , as a function of changing atmospheric pressure are shown in Fig. 3.

Although these equations for terminal velocity and kinetic energy provide important insight into the maximum possible velocity that a raindrop could attain as it passes through the atmosphere, and thus, the maximum energy that could be transferred to the surface for a given raindrop size, raindrop formation and evolution is more complicated than these simple equations can account for. Specifically, understanding more about how raindrops form, actual velocities at which they pass through the atmosphere, and how and why they might breakup is required for us to estimate maximum stable raindrop diameter and begin discussions about rainfall intensity and the erosive ability of the rainfall on early Mars.

Raindrops reaching the surface of a planet have a range of sizes as a result of their formation mechanism. Drops nucleate in clouds by condensation of water vapor onto extremely small nuclei. These nuclei can be dust particles derived from the surface due to the action of the wind or the results of the evaporation or disintegration of small meteoroids in the planetary atmosphere. The drops grow by ongoing water condensation and by collision-aided size sorting in turbulent eddies in the clouds (Falkovich et al., 2002). Upon saturation, droplets will leave the base of the cloud as precipitation. Droplets leaving the base of the cloud accelerate towards their terminal velocity, v_b , which is potentially reached when the weight of the droplet exactly balances the atmospheric drag force, as described above. However, as the drop velocity and the drag force acting on the raindrop increase, interaction between the stress distribution on the surface of the raindrop and the surface tension at the water-gas interface causes deformational instabilities (e.g. Villermaux and Bossa, 2009). For relatively large raindrops, this instability is reached before the terminal velocity is attained, and the drop

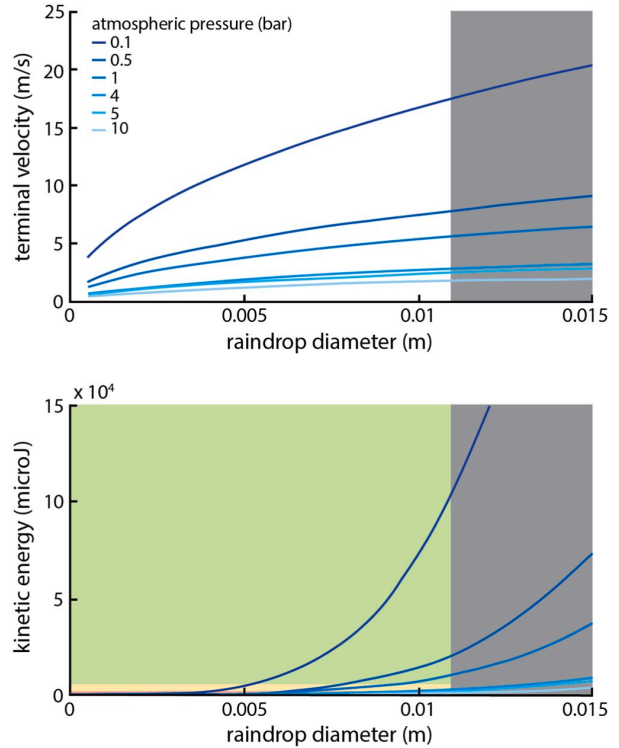


Fig. 3. Results of calculations for mathematical relationships between raindrop diameter and terminal velocity (top) and raindrop diameter and kinetic energy (bottom). Results are shown for atmospheric pressure ranging from 0.1 to 10 bar. In both plots, the region shaded gray represents conditions that are not possible on Mars because the raindrop diameter is larger than the maximum raindrop diameter that can pass through the Martian atmosphere and successfully reach the surface, 10.8 mm. In the bottom plot, the region shaded red represents kinetic energy values that are incapable of initiating transport of sedimentary particles (note that the area shaded red is very small), the region shaded yellow represents kinetic energy values that are incapable of initiating transport of sand-sized particles and larger, but not silt, and the region shaded green represents kinetic energy values that are capable of initiating transport of all sedimentary particles, including silt. These plots show that both rain splash-related erosion (sediment transport) could occur for the entire atmospheric pressure range considered here. Please note that the sedimentary particle sizes discussed here are within reason; we are not accounting for things as large as boulders, for example. (For interpretation of the references to color in this figure legend, the reader is referred to the web version of this article.)

breaks up catastrophically into a spectrum of smaller sizes. If the initial drop was large enough, some of these secondary drops may themselves be large enough to breakup before reaching their terminal velocity.

For any raindrop of diameter d that is falling at velocity v , this deformational instability occurs when the Weber number, We , equal to $[(\rho_a v^2 d) / \gamma]$ (where γ is surface tension), becomes greater than a critical value We_{crit} . We note that Kolev (2005, his chapter 8) discusses the influence of dynamic, viscous and surface tension forces on falling raindrops in great detail, and shows that the instability of falling raindrops also depends on the Ohnesorge number, Oh , equal to $[\mu / (\rho_a \gamma d)]^{1/2}$, where μ is the atmospheric gas viscosity. Oh must be less than ~ 4 to ensure drop instability, but for falling raindrops on both Earth and Mars this requirement is readily met with Oh being on the order of 10^{-2} to 10^{-4} , so we do not discuss Oh in any further detail, here. The value of the critical Weber number is variously taken to be close to 6 (Villermaux and Bossa, 2009), 8 (Craddock and Lorenz, 2017) or 12 (Kolev, 2005). We follow Craddock and Lorenz (2017) in assuming the value 8 for the Weber number, so the critical velocity to ensure breakup, or the ‘break-

up velocity', is $v_b = [(8 \gamma)/(\rho_a d)]^{1/2}$. Thus, the break-up velocity depends on the atmospheric density, ρ_a , and hence atmospheric pressure, and on the surface tension, γ , which depends weakly on atmospheric temperature. Over the 0–20 °C temperature range of relevance here, surface tension, γ , ranges from 0.0756 N/m to 0.0728 N/m (see https://www.engineeringtoolbox.com/water-surface-tension-d_597.html for a larger range of temperatures). We implement a value of 0.0728 N/m, again following Craddock and Lorenz (2017).

Therefore, the maximum velocity that a raindrop reaches as it passes through the atmosphere is either the terminal velocity, v_t , if $v_t < v_b$, or the break-up velocity, v_b , if $v_b < v_t$ and thus the raindrop will break-up before reaching terminal velocity. Table 1 shows the result of calculating both the terminal velocity, v_t , and the break-up velocity, v_b , for a range of raindrop diameters and atmospheric pressures/densities on early Mars. Consider the second column, for $d = 1$ mm. In every case the terminal velocity is much less than the break-up velocity, so for all of the atmospheric conditions shown, the maximum velocity that a 1 mm diameter raindrop would have reached as it passed through the atmosphere is its terminal velocity; 1 mm diameter raindrops will reach their terminal velocity without breaking up due to drop instabilities. Now, consider the final column, for $d = 15$ mm. In every case the terminal velocity is greater than the breakup velocity, so for all of the atmospheric conditions shown, the maximum velocity that a 15 mm diameter raindrop would have reached as it passed through the atmosphere is its break-up velocity; 15 mm diameter raindrops would have broken up due to drop instabilities before reaching their terminal velocity. Therefore, we show that larger raindrops (e.g. 15 mm diameter) will have a maximum velocity equal to their break-up velocity, while smaller raindrops (e.g. 1 mm diameter) will have a maximum velocity equal to their terminal velocity. Raindrops that are capable of reaching their terminal velocity without breaking up are stable as they pass through the atmosphere and raindrops that are not capable of reaching their terminal velocity are unstable as they pass through the atmosphere because they will break up. The critical result from Table 1 is that for every set of atmospheric conditions, the transition between stability and instability (reaching terminal velocity and not reaching terminal velocity) takes place at the same raindrop diameter, termed the maximum stable raindrop diameter, $d_{max} = 10.797$ mm (Table 1). The velocity marking the transition varies with the atmospheric conditions but, in contrast to Craddock and Lorenz (2017), we find that the maximum stable raindrop diameter is independent of atmospheric pressure. This result, that the maximum stable raindrop diameter, d_{max} , is independent of atmospheric pressure, is consistent with findings from previous numerical and experimental studies of water raindrop dynamics (e.g. Villermaux and Bossa, 2009) and with a model of methane raindrop behavior on Titan (Lorenz, 1993).

From the maximum stable raindrop diameter, d_{max} , we can estimate rainfall intensity. Rainfall intensity is useful for estimating regimes where rainfall exceeds infiltration capacity, permitting surface runoff. A parameterized relationship for rainfall intensity and median raindrop size has been developed for rainfalls on Earth (e.g. Marshall and Palmer, 1948) and follows:

Table 1

Variation of the terminal velocity, v_t , and breakup velocity, v_b , for a range of rain drop diameters, d , under Mars atmospheric pressures between 0.5 and 10 bar.

Atmospheric pressure (bar)	atmospheric density (kg/m ³)	d (mm)	0.5	1	3	5	7	9	10.797	12	15
0.5	0.903	v_t (m/s)	1.66	2.35	4.08	5.26	6.23	7.06	7.73	8.15	9.11
		v_b (m/s)	35.93	25.40	14.67	11.36	9.60	8.47	7.73	7.33	6.56
1	1.806	v_t (m/s)	1.18	1.66	2.88	3.72	4.40	4.99	5.47	5.76	6.44
		v_b (m/s)	25.40	17.96	10.37	8.03	6.79	5.99	5.47	5.19	4.64
4	7.225	v_t (m/s)	0.59	0.83	1.44	1.86	2.20	2.50	2.73	2.88	3.22
		v_b (m/s)	12.70	8.98	5.19	4.02	3.39	2.99	2.73	2.59	2.32
5	9.031	v_t (m/s)	0.53	0.74	1.29	1.66	1.97	2.33	2.44	2.58	2.88
		v_b (m/s)	11.36	8.04	4.64	3.59	3.04	2.68	2.44	2.32	2.07
10	18.062	v_t (m/s)	0.37	0.53	0.91	1.18	1.39	1.58	1.73	1.82	2.04
		v_b (m/s)	8.03	5.68	3.28	2.54	2.15	1.89	1.73	1.64	1.47

$$D_{50} = \alpha I^\beta$$

where D_{50} (mm) is the median raindrop size, approximated for simplicity to be half of the maximum stable raindrop diameter (following Craddock and Lorenz, 2017), I is rainfall intensity (measured in mm/h), and α and β are coefficients that have been approximated from empirical measurements of rainfalls on Earth to range from ~0.80–1.28 and 1.23–2.92, respectively (e.g. Craddock and Lorenz, 2017 and references therein). Thus, larger median raindrop sizes are correlated with more intense rainfall. However, because maximum stable raindrop diameter does not depend on atmospheric pressure (Table 1), the estimated median raindrop size within a given rainfall, D_{50} , will also be independent of atmospheric pressure, and, as a result, the rainfall intensity will be independent of atmospheric pressure, in contrast to the findings of Craddock and Lorenz (2017). Table 2 shows a calculation of rainfall intensity for different values of α and β .

Thus, our assessment based on this parameterized relationship for rainfall intensity suggests that a change in rainfall intensity as a function of time is not predicted to occur as a result of decreasing atmospheric pressure. Recall that such a change in rainfall intensity is required to explain the shift from a diffusive to advective rainfall-related erosional regime in a long-lived “warm and wet” climate (Craddock and Lorenz, 2017). Our results suggest that either (1) the long-lived climate was “warm and wet” and a mechanism other than decreasing atmospheric pressure was responsible for the shift in rainfall intensity and rainfall-related erosional regime, or (2) the long-lived climate was “cold and icy” and the peak in fluvial and lacustrine activity and advective erosion in the LN-EH was due to punctuated heating, ice melting, and surface runoff, not rainfall.

Table 2

Results of calculations to estimate rainfall intensity as a function of raindrop size. We characterize rainfall intensity in terms of “light” and “moderate” rain (Craddock and Lorenz, 2017; Kittredge, 1948)^a.

Maximum raindrop size (mm)	Median raindrop size (mm)	Rainfall intensity (mm/h)			
		$\alpha = 0.8,$ $\beta = 1.23$	$\alpha = 1.28,$ $\beta = 1.23$	$\alpha = 0.8,$ $\beta = 2.92$	$\alpha = 1.28,$ $\beta = 2.92$
10.8	5.4	4.9	3.1	2.2	1.4

^a Notes:

- (1) Kittredge (1948) focused on terrestrial rainfall rates with respect to erosion in highly-vegetated regions and we acknowledge that a more useful method for characterizing rainfall intensity be with respect to infiltration capacity of the Martian regolith instead of highly-vegetated regions on Earth for many reasons, including the lack of vegetation on the Martian surface.
- (2) This approximation of rainfall intensity does not account for intermittency in rainfall events; this method only predicts an average rainfall rate. Nonetheless, we see that both light and moderate rainfall are possible given the range of possible values for α and β . Note that rainfall intensity does not depend on atmospheric pressure.
- (3) “Light rain” is defined as rainfall rates 1–3.4 mm/h and “moderate rain” is defined as rainfall rates >3.4 mm/h.

However, it is important to note that this parameterized relationship comes from observations of rainfall of varying intensity and measurements of raindrop counts on Earth (e.g. Marshall and Palmer, 1948; Bennett et al., 1984), has been confirmed for rainfall on Earth when averaged over time and space (Brodie and Rosewell, 2007), and has been confirmed with numerical experiments of rainfall on Earth (e.g. Villermaux and Bossa, 2009). Despite this confirmation of the accuracy of this parameterized relationship for describing rainfall on Earth, we must reiterate the potential importance of the fact that this relationship was derived under terrestrial conditions based on rainfall on Earth. As such, we should revisit the mathematical equation that was simplified and approximated to arrive at this parameterized relationship ($D_{50} = \alpha D^\beta$) in order to confirm that this relationship can be directly applied to Mars and, more specifically, that the constants α and β do not actually depend on atmospheric pressure (we already confirmed above that the only other variable, D_{50} , does not depend on atmospheric pressure). In other words, we look to confirm our finding that rainfall intensity does not depend on atmospheric pressure. To do this, we can revisit the mathematical derivation of rainfall intensity, which is shown in equations 4 and 5 in Villermaux and Bossa (2009).

Specifically, rainfall intensity is mathematically described as the integral over raindrop diameter of the number of drops of a given size, times the volume of a raindrop of a given size, times the free-fall velocity (the maximum velocity) of a raindrop of a given size passing through the atmosphere (e.g. Villermaux and Bossa, 2009). Equation 5 from Villermaux and Bossa (2009) shows that rainfall intensity can be expressed in the following way (with variable names updated to match the conventions that we have implemented here):

$$I = n_0 \frac{\pi}{6} \sqrt{\frac{\rho_{\text{water}}}{\rho_a}} \sqrt{g D_{50}} \int x^{7/2} p(x) dx$$

where n_0 represents the average spatial density of raindrops and depends on temperature (Villermaux and Bossa, 2009 and references therein), and the integral is a term approximately equal to the raindrop size distribution. Of course, the derivation of maximum/median stable raindrop diameter and the parameterized relationship for rainfall intensity have already confirmed that rainfall intensity depends on gravity. The new information that is brought to light here is that rainfall intensity also depends on $\sqrt{\frac{\rho_{\text{water}}}{\rho_a}}$; rainfall intensity does in fact depend on atmospheric pressure. This atmospheric pressure term originates from the maximum velocity term in the integral in equation 4 from Villermaux and Bossa (2009), because maximum raindrop velocity depends on atmospheric pressure (as we have shown previously in our derivations of v_t and v_b , as well). Studies of rainfall intensity on Earth have assumed $\sqrt{\frac{\rho_{\text{water}}}{\rho_a}}$ to be constant because the variation in atmospheric pressure on present-day Earth is so small that the term varies negligibly (e.g. Villermaux and Bossa, 2009); this term is canonically wrapped in what we refer to as α in the parameterized relationship for rainfall intensity discussed above. Such an assumption is appropriate for assessments of rainfall on present-day Earth; however, when considering how atmospheric pressure has changed over billions of years on Mars, we cannot assume that the variation in this term would be negligible. Specifically, if we consider atmospheric pressure ranging from 0.5 to 10 bar (0.903 kg/m³ to 18.062 kg/m³), then $\sqrt{\frac{\rho_{\text{water}}}{\rho_a}}$ would range from 33 to 7.5, a factor of ~ 5 difference. This relationship shows that, if all else remains constant, more intense rainfall would have in fact occurred under lower atmospheric pressure conditions than under higher atmospheric pressure conditions (e.g. as atmospheric pressure decreased in the Noachian, rainfall intensity may have increased). In order to fully understand whether rainfall intensity could increase substantially enough to cause variations in erosive style, though, would require additional information that is not available at this time. Specifically, raindrop size distributions and estimates for n_0 on Earth come from

observations and measurements, which cannot be made for martian rainfall and have not yet been modeled. However, a quick speculation follows. As atmospheric pressure decreases, interactions between molecules in the atmosphere would also become less common, as a result potentially decreasing the integral of the drop size distribution and the value of n_0 . Therefore, although the value of $\sqrt{\frac{\rho_{\text{water}}}{\rho_a}}$ would increase, the values of n_0 and the integral term should systematically decrease. Whether these factors completely counteract one another, however, is yet to be determined.

We can summarize our discussion about rainfall intensity with two key points:

- (1) By implementing the parameterized relationship for rainfall intensity that has been proven to be appropriate for rainfall on Earth, we find that rainfall intensity does not depend on atmospheric pressure. This is true because maximum stable raindrop diameter does not depend on atmospheric pressure and, also for this reason, is in contrast to the finding of Craddock and Lorenz (2017). This finding suggests that decreasing atmospheric pressure on early Mars would not have directly led to increased rainfall intensity.
- (2) We have explored further the equations that originally led to this parameterized relationship for rainfall on Earth and find that rainfall intensity does actually depend on atmospheric pressure, albeit in a different way than assumed by previous studies (e.g. Craddock and Lorenz, 2017). However, the exact nature of the relationship between rainfall intensity and atmospheric pressure cannot be estimated at this time because there are other variables in the equation that are currently unknown for putative martian rainfalls.

5. Discussion and conclusions

The geomorphic evidence for rainfall in the Noachian has been interpreted to mean that there were two distinct rainfall-related erosional regimes on Mars, including a rain splash-dominated diffusive erosional regime in the Early-to-Mid Noachian and a runoff-dominated advective erosional regime in the LN-EH (e.g. Craddock and Lorenz, 2017). However, many recent climate modeling studies have had difficulty reproducing a climate scenario in which abundant rainfall occurs (e.g. Forget et al., 2013; Wordsworth et al., 2013); rainfall does not occur in a “cold and icy” climate and rainfall is negligible in greenhouse-heated and high altitude-cloud heated transient warm climates that may have occurred in an otherwise “cold and icy” climate. In this research, we set out to test the hypothesis that the two Noachian rainfall-related erosional regimes can be reconciled by a long-lived climate that was “warm and wet” with continuous rainfall because rainfall intensity would have changed through time as a function of decreasing atmospheric pressure, leading to the different rainfall-related erosional regimes (as described by Craddock and Lorenz, 2017). This proposed relationship between rainfall intensity and atmospheric pressure specifically suggests that higher atmospheric pressures are consistent with rain splash-dominated erosion and lower atmospheric pressures are consistent with runoff-dominated erosion (down to a given pressure threshold where temperatures conducive to liquid water would no longer be possible). We mathematically test this hypothesis by determining whether rainfall intensity depends on atmospheric pressure. This is critical for our understanding of the evolution of the martian hydrological cycle and for placing tighter constraints on the hydrological system characteristics that climate models must reproduce.

Our findings are summarized below.

1. Based on our calculations of the kinetic energy transferred as raindrops collide with the surface, we find that raindrops on Mars would

- be capable of transferring sufficient energy to initiate sediment transport regardless of atmospheric pressure (rain splash; Fig. 3).
- Maximum stable raindrop size does not depend on atmospheric pressure. This is in contrast to the findings of Craddock and Lorenz (2017).
 - A parameterized relationship for rainfall intensity has been identified on Earth based on experiments, observations, and mathematical approaches. When we apply this relationship to Mars, we find that rainfall intensity does not vary as a function of atmospheric pressure. This finding is inconsistent with the hypothesis that rainfall intensity changed as atmospheric pressure declined through time in a long-lived “warm and wet” Noachian climate with rainfall throughout the Noachian. We note that the constants in this parameterized relationship come from observations of rainfall on present-day Earth and that appropriate assessments of these constants for early Mars is not currently possible. However, these constants do depend on atmospheric pressure in a way that has previously not been considered in assessments of martian rainfall, and thus, this topic warrants future study. Future work should aim to better constrain the parameters in the original mathematical equation for rainfall intensity (e.g. Villiermaux and Bossa, 2009) in order to better understand the relationship between rainfall intensity and atmospheric pressure, which is more complicated than the simple parameterized relationship suggests.

Many outstanding questions remain, including:

- If the long-lived Noachian climate was “warm and wet”, what mechanism can explain the apparent shift in rainfall intensity from the Early-to-Mid Noachian to the LN-EH?
- If the long-lived Noachian climate was “cold and icy”, what mechanism was responsible for producing a period of intense fluvial and lacustrine activity in the LN-EH?
- Is melting of surface snow/ice and runoff capable of producing sufficient advective erosion to explain the formation of the valley networks and lakes, or is rainfall required?
- How can continuous diffusive erosion throughout the Noachian be reconciled with a “cold and icy” climate in the absence of rainfall?

Declaration of competing interest

The authors declare that they have no known competing financial interests or personal relationships that could have appeared to influence the work reported in this paper.

Acknowledgements

This work was supported by NASA Headquarters under the NASA Earth and Space Science Fellowship Program for AMP; Grant 90NSSC17K0487, and the Mars Express High Resolution Stereo Camera Team (HRSC) (JPL 1488322) for JWH. LW thanks the Leverhulme Trust for support through an Emeritus Fellowship. The authors thank the reviewers for helpful feedback, including Dr. Michael Mischna and Dr. Edwin Kite. The authors also thank Ben Boatwright for helpful discussions.

References

Batalha, N., Kopparapu, R., Haqq-Misra, J., Kasting, J., 2016. Climate cycling on early Mars caused by the carbonate-silicate cycle. *Earth Planet. Sci. Lett.* 455, 7–13. <https://doi.org/10.1016/j.epsl.2016.08.044>.

Bennett, J., Fang, D., Boston, R., 1984. Relationships between N_0 and A for Marshall-Palmer type raindrop-size distributions. *J. Clim. Appl. Meteorol.* 23, 768–771.

Bouley, S., Baratoux, D., Paulien, N., Missenard, Y., Saint-Bezar, B., 2018. The revised tectonic history of Tharsis. *Earth Planet. Sci. Lett.* 488, 126–133. <https://doi.org/10.1016/j.epsl.2018.02.019>.

Brodie, I., Rosewell, C., 2007. Theoretical relationships between rainfall intensity and kinetic energy variants associated with stormwater particle washoff. *J. Hydrol.* 340 (1–2), 40–47. <https://doi.org/10.1016/j.jhydrol.2007.03.019>.

Cabrol, N., Grin, E., 1999. Distribution, classification, and ages of Martian impact crater lakes. *Icarus* 142 (1), 160–172. <https://doi.org/10.1006/icar.1999.6191>.

Craddock, R., Howard, A., 2002. The case for rainfall on a warm, wet early Mars. *Journal of Geophysical Research: Planets* 107 (E11), 5111. <https://doi.org/10.1029/2001JE001505>.

Craddock, R., Lorenz, R., 2017. The changing nature of rainfall during the early history of Mars. *Icarus* 293, 172–179. <https://doi.org/10.1016/j.icarus.2017.04.013>.

Craddock, R., Maxwell, T., Howard, A., 1997. Crater morphometry and modification in the Sinus Sabaeus and Margaritifer Sinus regions of Mars. *Journal of Geophysical Research: Planets* 102 (E6), 13321–13340. <https://doi.org/10.1029/97JE01084>.

Craddock, R., Bandeira, L., Howard, A., 2018. An assessment of regional variations in Martian modified impact crater morphology. *Journal of Geophysical Research: Planets* 123 (3), 763–779. <https://doi.org/10.1002/2017JE005412>.

Falkovich, G., Fouxon, A., Stepanov, M., 2002. Acceleration of rain initiated by cloud turbulence. *Nature* 419, 151–154.

Fassett, C., Head, J., 2008a. The timing of martian valley network activity: constraints from buffered crater counting. *Icarus* 195 (1), 61–89. <https://doi.org/10.1016/j.icarus.2007.12.009>.

Fassett, C., Head, J., 2008b. Valley network-fed, open-basin lakes on Mars: distribution and implications for Noachian surface and subsurface hydrology. *Icarus* 198 (1), 37–56. <https://doi.org/10.1016/j.icarus.2008.06.016>.

Fassett, C., Head, J., 2011. Sequence and timing of conditions on early Mars. *Icarus* 211 (2), 1204–1214. <https://doi.org/10.1016/j.icarus.2010.11.014>.

Fastook, J., Head, J., 2015. Glaciation in the Late Noachian Icy Highlands: Ice accumulation, distribution, flow rates, basal melting, and top-down melting rates and patterns. *Planet. Space Sci.* 106, 82–98.

Forget, F., Pierrehumbert, R., 1997. Warming early Mars with carbon dioxide clouds that scatter infrared radiation. *Science* 278 (5341), 1273–1276. <https://doi.org/10.1126/science.278.5341.1273>.

Forget, F., Wordsworth, R., Millour, E., Madeleine, J.-B., Kerber, L., Leconte, J., et al., 2013. 3D modelling of the early Martian climate under a denser CO₂ atmosphere: temperatures and CO₂ ice clouds. *Icarus* 222 (1), 81–99. <https://doi.org/10.1016/j.icarus.2012.10.019>.

Forsberg-Taylor, N., Howard, A., Craddock, R., 2004. Crater degradation in the Martian highlands: morphometric analysis of the Sinus Sabaeus region and simulation modeling suggest fluvial processes. *Journal of Geophysical Research: Planets* 109 (E5), E05002. <https://doi.org/10.1029/2004JE002242>.

Goudge, T., Aureli, K., Head, J., Fassett, C., Mustard, J., 2015. Classification and analysis of candidate impact crater-hosted closed-basin lakes on Mars. *Icarus* 260, 346–367. <https://doi.org/10.1016/j.icarus.2015.07.026>.

Halevy, I., Head, J., 2014. Episodic warming of early Mars by punctuated volcanism. *Nat. Geosci.* 7 (12), 865–868. <https://doi.org/10.1038/ngeo2293>.

Head, J., Marchant, D., 2014. The climate history of early Mars: insights from the Antarctic McMurdo Dry Valleys hydrologic system. *Antarct. Sci.* 26 (6), 774–800.

Head, J., Forget, F., Wordsworth, R., Turbet, M., Cassanelli, J., Palumbo, A., 2018. Two oceans on Mars?: history, problems and prospects. In: 49th Lunar and Planetary Science Conference, p. 2194 (The Woodlands, TX).

Holm, N., Oze, C., Mousis, O., Waite, J., Guilbert-Lepoutre, A., 2015. Serpentinization and the formation of H₂ and CH₄ on celestial bodies (planets, moons, comets). *Astrobiology* 15 (7), 587–600. <https://doi.org/10.1089/ast.2014.1188>.

Howard, A., 2007. Simulating the development of Martian highland landscapes through the interaction of impact cratering, fluvial erosion, and variable hydrologic forcing. *Geomorphology* 91 (3), 332–363. <https://doi.org/10.1016/j.geomorph.2007.04.017>.

Howard, A., Moore, J., Irwin, R., 2005. An intense terminal epoch of widespread fluvial activity on early Mars: 1. Valley network incision and associated deposits. *Journal of Geophysical Research: Planets* 110 (E12), 12. <https://doi.org/10.1029/2005JE002459>.

Hynek, B., Beach, M., Hoke, M., 2010. Updated global map of Martian valley networks and implications for climate and hydrologic processes. *Journal of Geophysical Research: Planets* 115 (E9), E09008. <https://doi.org/10.1029/2009JE003548>.

Irwin, R., Howard, A., Craddock, R., Moore, J., 2005. An intense terminal epoch of widespread fluvial activity on early Mars: 2. Increased runoff and paleolake development. *Journal of Geophysical Research: Planets*. [https://doi.org/10.1029/2005JE002460@10.1002/\(ISSN\)2169-9100.EARLYMARS1](https://doi.org/10.1029/2005JE002460@10.1002/(ISSN)2169-9100.EARLYMARS1).

Irwin, R., Craddock, R., Howard, A., Flemming, H., 2011. Topographic influences on development of Martian valley networks. *J. Geophys. Res.* 116 (E2), E02005 <https://doi.org/10.1029/2010JE003620>.

Johnson, S., Mischna, M., Grove, T., Zuber, M., 2008. Sulfur-induced greenhouse warming on early Mars. *J. Geophys. Res.* 113, E08005 <https://doi.org/10.1029/2007JE002962>.

Jones, K., 1974. Evidence for an episode of crater obliteration intermediate in Martian history. *J. Geophys. Res.* 79 (26), 3917–3931. <https://doi.org/10.1029/JB079i026p03917>.

Kasting, J., 1991. CO₂ condensation and the climate of early Mars. *Icarus* 94 (1), 1–13. [https://doi.org/10.1016/0019-1035\(91\)90137-1](https://doi.org/10.1016/0019-1035(91)90137-1).

Kavanagh, L., Goldblatt, C., 2015. Using raindrops to constrain past atmospheric density. *Earth Planet. Sci. Lett.* 413, 51–58. <https://doi.org/10.1016/j.epsl.2014.12.032>.

Kerber, L., Forget, F., Wordsworth, R., 2015. Sulfur in the early martian atmosphere revisited: experiments with a 3-D global climate model. *Icarus* 261, 133–148.

Kite, E., Halevy, I., Kahre, M., Wolff, M., Manga, M., 2013. Seasonal melting and the formation of sedimentary rocks on Mars, with predictions for the Gale Crater mound. *Icarus* 223, 181–210.

- Kite, E., Gao, P., Goldblatt, C., Mischna, M., Mayer, D., Yung, Y., 2017. Methane bursts as a trigger for intermittent lake-forming climates on post-Noachian Mars. *Nat. Geosci.* 10 (10), 737–740. <https://doi.org/10.1038/ngeo3033>.
- Kite, E., Steele, J., Mischna, M., 2019. Aridity enables warm climates on Mars. In: 50th Lunar and Planetary Science Conference (p. Abstract 1360). The Wood.
- Kittredge, J., 1948. *Forest Influences: The Effects of Woody Vegetation on Climate, Water, and Soil, With Applications to the Conservation of Water and the Control of Floods and Erosion*. McGraw-Hill Book Co., Inc, New York, USA.
- Kolev, N., 2005. *Multiphase Flow Dynamics 2 – Thermal and Mechanical Interactions*. Springer-Verlag, p. 699.
- Lorenz, R., 1993. The life, death and afterlife of a raindrop on Titan. *Planet. Space Sci.* 41 (9), 647–655.
- Madeleine, J.-B., Forget, F., Millour, E., Navarro, T., Spiga, A., 2012. The influence of radiatively active water ice clouds on the Martian climate. *Geophys. Res. Lett.* 39 (23) <https://doi.org/10.1029/2012GL053564>.
- Madeleine, J.-B., Head, J., Forget, F., Navarro, T., Millour, E., Spiga, A., et al., 2014. Recent ice ages on Mars: the role of radiatively active clouds and cloud microphysics. *Geophys. Res. Lett.* 41 (14), 4873–4879. <https://doi.org/10.1002/2014GL059861>.
- Marshall, J., Palmer, W., 1948. The distribution of raindrops with size. *J. Meteorol.* 5, 165–166.
- Matsubara, Y., Howard, A.D., Goehenour, J.P., 2013. Hydrology of early Mars: valley network incision. *Journal of Geophysical Research: Planets* 118 (6), 1365–1387. <https://doi.org/10.1002/jgre.20081>.
- Mischna, M., Baker, V., Milliken, R., Richardson, M., Lee, C., 2013. Effects of obliquity and water vapor/trace gas greenhouses in the early martian climate. *Journal of Geophysical Research: Planets* 118, 560–576.
- Mischna, M., Kite, E., Steele, L., 2019. Aridity enables warm climate on Mars. In: Ninth International Conference on Mars. Pasadena, CA. Abstract 6042.
- Mischna, M., Kasting, J., Pavlov, A., Freedman, R., 2000. Influence of carbon dioxide clouds on early martian climate. *Icarus* 145 (2), 546–554. <https://doi.org/10.1006/icar.2000.6380>.
- Palumbo, A., Head, J., 2018a. Early Mars climate history: characterizing a “warm and wet” Martian climate with a 3D global climate model and testing geological predictions. *Geophys. Res. Lett.* 45 <https://doi.org/10.1029/2018GL079767>.
- Palumbo, A., Head, J., 2018b. Impact cratering as a cause of climate change, surface alteration, and resurfacing during the early history of Mars. *Meteorit. Planet. Sci.* 53 (4), 687–725. <https://doi.org/10.1111/maps.13001>.
- Palumbo, A., Head, J., Wordsworth, R., 2018. Late Noachian icy highlands climate model: exploring the possibility of transient melting and fluvial/lacustrine activity through peak annual and seasonal temperatures. *Icarus* 300, 261–286.
- Ramirez, R., 2017. A warmer and wetter solution for early Mars and the challenges with transient warming. *Icarus* 297, 71–82. <https://doi.org/10.1016/j.icarus.2017.06.025>.
- Ramirez, R., Craddock, R., 2018. The geological and climatological case for a warmer and wetter early Mars. *Nature Geoscience Perspective* 11, 230–237. <https://doi.org/10.1038/s41561-018-0093-9>.
- Ramirez, R., Kopparapu, R., Zuger, M., Robinson, T., Freedman, R., Kasting, J., 2014. Warming early Mars with CO₂ and H₂. *Nat. Geosci.* 7 (1), 59–63. <https://doi.org/10.1038/ngeo2000>.
- Segura, T., Toon, O., Colaprete, A., 2008. Modeling the environmental effects of moderate-sized impacts on Mars. *Journal of Geophysical Research: Planets* 113 (E11), E11007. <https://doi.org/10.1029/2008JE003147>.
- Som, S., Catling, D., Harnmeijer, J., Polivka, P., Buick, R., 2012. Air density 2.7 billion years ago limited to less than twice modern levels by fossil raindrop imprints. *Nature* 484 (7394), 359–362. <https://doi.org/10.1038/nature10890>.
- Toon, O., Segura, T., Zahnle, K., 2010. The formation of Martian river valleys by impacts. *Annu. Rev. Earth Planet. Sci.* 38, 303–322.
- Turbet, M., Tran, H., Pirali, O., Forget, F., Boulet, C., Hartmann, J.-M., 2019. Far infrared measurements of absorptions by CH₄ + CO₂ and H₂ + CO₂ mixtures and implications for greenhouse warming on early Mars. *Icarus* 321, 189–199. <https://doi.org/10.1016/j.icarus.2018.11.021>.
- Urata, R., Toon, O., 2013. Simulations of the martian hydrologic cycle with a general circulation model: implications for the ancient martian climate. *Icarus* 226 (1), 229–250. <https://doi.org/10.1016/j.icarus.2013.05.014>.
- Villermaux, E., Bossa, B., 2009. Single-drop fragmentation determines size distribution of raindrops. *Nature Physics* 5, 697–702.
- Warren, A., Kite, E., Williams, J.-P., Horgan, B., 2019. Multi-Gyr history of Mars’ CO₂-dominated atmosphere: New data and a new synthesis. In: Ninth International Conference on Mars (p. Abstract 6112). Pasadena, CA.
- Wordsworth, R., 2016. The climate of early Mars. *Annu. Rev. Earth Planet. Sci.* 44 (1), 381–408. <https://doi.org/10.1146/annurev-earth-060115-012355>.
- Wordsworth, R., Forget, F., Millour, E., Head, J.W., Madeleine, J.-B., Charnay, B., 2013. Global modelling of the early martian climate under a denser CO₂ atmosphere: water cycle and ice evolution. *Icarus* 222, 1–19.
- Wordsworth, R., Kerber, L., Pierrehumbert, R., Forget, F., Head, J., 2015. Comparison of “warm and wet” and “cold and icy” scenarios for early Mars in a 3-D climate model. *Journal of Geophysical Research: Planets* 120, 1201–1219.
- Wordsworth, R., Kalugina, Y., Lokshtanov, S., Vigin, A., Ehlmann, B., Head, J., et al., 2017. Transient reducing greenhouse warming on early Mars. *Geophys. Res. Lett.* 44 (2) <https://doi.org/10.1002/2016GL071766>, 2016GL071766.